Liquid metal slingshot-a self-propelled and controllable motion

Zhiping Yuan[1], Xudong Zhang[2], Huimin Hou[1], Zhifeng Hu[1], Xiaomin Wu[1*], Jing Liu[2,3*]

[1]Key Laboratory for Thermal Science and Power Engineering of Ministry of Education, Department of Energy and Power Engineering, Tsinghua University, Beijing 100084, China
[2]Key Lab of Cryogenics, Technical Institute of Physics and Chemistry, Chinese Academy of Sciences, Beijing 100190, China;
[3]Department of Biomedical Engineering, School of Medicine, Tsinghua University, Beijing 100084, China

Abstract: This paper report a new kind of self-propelled motion of liquid metal droplet, which driven by surface tension not rely on any external forces field. It can control the speed and direction of motion just like a projectile fired by a slingshot. The liquid metal droplet is the projectile, and a substrate surface serves as the bowstring. Liquid metal droplet accumulates energy through contact with the substrate and then induces the firing action through coalescence. Changing the shape of the bowstring can make the bowstring accumulate more efficient energy so that the projectile would obtain a higher projection velocity. Furthermore, the force between the liquid metal droplet and the bowstring will also thus be changed so that the projectile can be fired in an expected direction. This self-propelled and controllable motion is of great significance for the application of liquid metals in nanomachines, rapid cooling, targeted therapy, and others.

Keywords: Self-propelled, liquid metal, surface tension, controllable

Table of Contents:

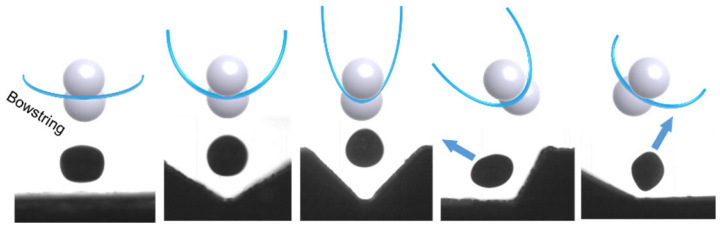

INTRODUCTION

Liquid metal has essential applications in 3D printing[1-3], nanomachine[4, 5], deformable metal material [6-8], microfluidic chip [9-11], and rapid cooling[12-15], because of its excellent conductivity, thermal conductivity, and fluidity. Many of these applications depend on the motion of the liquid metal droplet, and the triggering of these motions requires additional fields, typically, such as magnetic field[9, 16], and electricity[17, 18]. Although these driving mechanisms are well understood, these motion processes are not self-propelled, but rely on the driving of other devices, which limits the application potential of the liquid metal.

Surface tension can drive aqueous liquids to produce a series of self-propelled motion phenomena on a micro-scale. For instance, the directional transport of droplets occurs on a surface with wetting

gradient or with anisotropic structure[19-22]; the self-propelled jumping and sweeping of condensing droplets on the superhydrophobic surface[23-26], the rotation, and curling of the ice water mixture in a superhydrophobic surface or a slippery surface[27, 28]. These self-propelled motion have high scientific value and application value and are still the research hotspot at present. The surface tension coefficient of liquid metal is higher than that of water fluid, and its dynamic viscosity is lower than that of water fluid, so the effect of surface tension on its motion should be more significant. Especially in the Micro-nano scale, the surface tension may replace the electric force and magnetic force as the driving force of liquid metal movement. In contrast with the current hot research on the self-propelled motion of aqueous liquids, the research on self-propelled of liquid metals needs more attention.

In this study, a self-propelled and controllable motion of liquid metal droplets is first reported. Liquid metal droplets can motion independent of the external force field， and can optionally change the projection direction and velocity by changing the shape of the bowstring (substrate surface). Combined with experiments and simulation, the firing mechanism is analyzed, and a theoretical model of the relationship between the projection velocity, direction, and bowstring shape is established.

RESULT AND DISCUSSION

Materials and methods The liquid metal used in this paper is gallium indium alloy (weight percentage, Ga 90 %, In 10 %, 6280 kg/m^3) with high surface tension (0.65 N/m) and low viscosity (2.7e-7 N·s/m^2). A microsyringe is used to produce liquid metal droplets of suitable size on the substrate surface, and these two droplets are gently stirred to coalesce and fire. In order to prevent the oxide layer on the liquid metal surface blocking the flow of the liquid metal, the experiments were carried out in a 0.5 mol/L NaOH solution. The materials of the substrate surface used in the experiments include silicon wafer, glass, and aluminum surface modified by 1H,1H,2H,2H-Perfluorodecyltriethoxysilane (Al-FAS). The purpose of using FAS to modify the aluminum surface is to prevent the double electric layer from blocking the coalescence of the droplets and also delaying the reaction between Al and NaOH. In the modification step, the aluminum surface is polished with 1000 grit sandpaper, then placed in 0.1 mol/L FAS solution for 30 minutes, and then dried in an oven at 100°C for 30 minutes. The contact angle of liquid metal droplets on Al-FAS, glass, and silicon wafer substrate surface is about 140° to 150°. The simulation uses the interFoam solver based on VOF in OpenFOAM. The size of the simulation domain is 6mm×6mm×6 mm, and the mesh resolution is 200×200×200. The substrate surface is set as the superhydrophobic non-slip boundary condition, and the other is the pressure outlet boundary condition. The physical parameters are the same as the experimental parameters. More detailed experimental and simulation can be seen in our previous research [11, 25, 29].

Fire mechanism Fig. 1 shows the coalescence of two liquid metal droplets on the Al-FAS substrate (Case 1, see Video S1). At the initial stage of coalescence (Stage I), a liquid bridge (0.0 ms-1.00 ms) is generated at the contact position of the two droplets. Then, the liquid bridge expands under the surface tension and finally contacts the substrate (1.00 ms-2.00 ms). At the later stage of coalescence (Stage II), the liquid bridge expands further, and the droplets begin to contract towards the middle. The reaction force of the substrate surface to the liquid bridge makes the droplets depart from the substrate surface (4.00 ms-8.50 ms). After the droplet departure off the surface, it rises with

deformation (8.50 ms -17.00 ms).

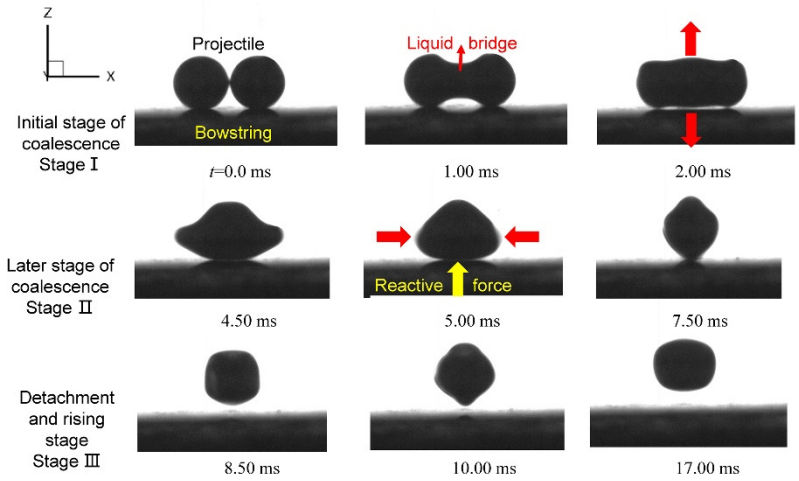

Fig. 1. The morphology evolution of liquid metal droplet with time in case 1. The volume of a single droplet is 2.5 μl, and the radius is 842 μm. The velocity of the droplets when they depart the surface is about 0.160 m/s. Two groups of red arrows in the figure respectively indicate the expansion of the liquid bridge and the contraction of the droplets.

At the initial impression, the experimental results in Fig. 1 will cause confusion because we do not think that energy is stored on a straight bowstring in general, and then a straight bowstring cannot fire the projectile. The energy stored by the bowstring in the liquid metal slingshot is the surface energy, while that of the ordinary slingshot is the elastic potential energy. This difference can be revealed by analyzing the energy change of the liquid metal slingshot. We use simulation to study the process of energy conversion because it is difficult to measure in the experiment. The change in projection kinetic energy ΔE_k from the initial state is calculated as follows:

$$\Delta E_k = \frac{1}{2} m(u^2 + v^2 + w^2) \tag{1}$$

where m is the mass of the droplet, u, v, w are the average mass velocities in X, Y, Z directions, respectively. The change of surface energy consists of three parts: the change of surface energy of liquid metal-NaOH solution interface ΔE_{ml}, the change of surface energy of liquid metal-substrate interface ΔE_{ms}, and the change of surface energy of substrate interface-NaOH solution ΔE_{sl}, respectively. The surface energy change equates to the product of the change of surface area and the coefficient of surface tension.

$$\Delta E_s = \delta_{ml}\Delta A_{ml} + \delta_{ms}\Delta A_{ms} + \delta_{sl}\Delta A_{sl} \tag{2}$$

where δ and ΔA are the surface tension coefficient and area change of three interfaces, respectively. The area change values of metal-substrate interface and solution-substrate interface are equal, and these two energy changes are marked ΔE_{msl} together. According to Young's equation, *Eq*(2) can be written as follows:

$$\Delta E_s = \delta_{ml}\Delta A_{ml} - \delta_{ml}\cos(\theta)\Delta A_{ms} \tag{3}$$

where θ is the contact angle. The ΔA_{ml} of two small globular droplets coalescence to a big globular droplet can be defined as:

$$\Delta A_{ml}=4\pi R^2\left[(1-\cos(\theta))-\left(2-\frac{(1+\cos(\theta))^2(2-\cos(\theta))}{2}\right)^{2/3}\right] \tag{4}$$

where R is droplet radius. The ΔA_{ms} can be defined as:

$$\Delta A_{ms}=\frac{4R^2\sin(\theta)}{\sin(\theta_{bb}/2)}\times\left[\begin{array}{l}\sin(\theta_{bb}/2)\sin(\theta)\operatorname{acos}\left(\dfrac{\cos(\theta_{bb}/2)\cos(\theta)}{\sin(\theta_{bb}/2)\sin\theta}\right)-\\ \cos(\theta_{bb}/2)\cos(\theta)\left(\dfrac{\sin(\theta)^2+\sin(\theta_{bb}/2)^2-1}{\sin(\theta_{bb}/2)^2\sin(\theta)^2}\right)^{(1/2)}\end{array}\right] \tag{5}$$

where θ_{bb} is the angle between the two bowstrings, the contact angle is taken as the median value 145° of contact angle of three surfaces. Fig. 2 shows the surface energy and projection kinetic energy of case1 in Fig. 1 as a function of time. The E_{ml} decreases at the initial stage of coalescence (stage I) and increases slightly at the stage of contraction and detachment (stage II). For the E_{msl}, the generation and expansion of liquid metal bridge make the metal fluid concentrate in the middle, and the contact surface between liquid metal and substrate decreases until the liquid metal bridge contacts the substrate surface, resulting in it decrease first and then increase (stage I). Then, the E_{msl} decrease with the droplet shrinking (stage II). The projection kinetic energy of liquid metal droplets hardly changes in stage I, but increases rapidly in stage II, and decreases dramatically before departure the substrate. When the droplet departs off the surface, that is the beginning of stage III, the surface energy E_{msl} can be released entirely. In contrast, the surface energy of the liquid metal-solution cannot be released entirely due to the large deformation of the droplet, which is only about 60% of the ideal release amount *Eq*.4, and the effective release amount of E_{ml} is almost the same as the release amount of E_{msl}.

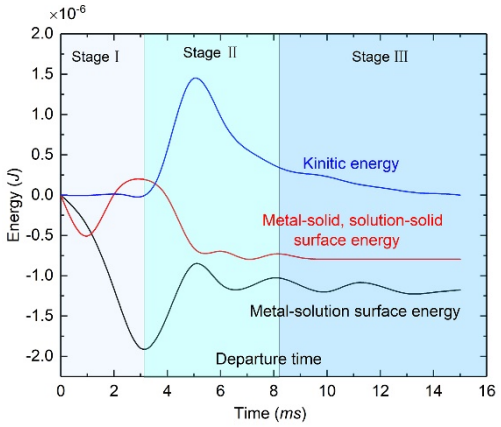

Fig. 2. Change of surface energy and projection kinetic energy versus time

Fig. 3 shows the change of projection velocity of the liquid metal droplet on three substrates of Al-FAS, silicon wafer, and glass with droplet radius, respectively. We can see that the projection velocity of liquid metal droplets decreases with an increase of radius, and do not affect by substrate materials. According to the dimensionless processing methods of impact, rebound and coalescence of a water droplet in the past studies, the dimensionless processing of projection velocity is defined as [30-32]:

$$v^*=v/(\delta_{ml}/\rho R)^{1/2} \tag{6}$$

where ρ is the density of the liquid metal, v, and v^* are the measured velocity and the dimensionless velocity, respectively. As shown in Fig. 3, for the projection of two equal liquid metal droplets, the dimensionless projection velocity is almost independent of the droplet radius and substrate. According to this, we can define the projection velocity of the liquid metal projectile as:

$$v = C_0(\delta_{ml} / \rho R)^{1/2} \tag{7}$$

when the shape of the bowstring is straight, C_0 is 0.45~0.48.

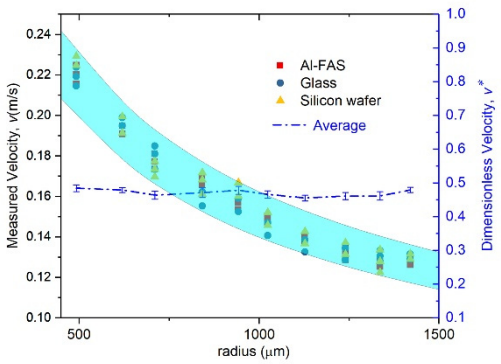

Fig. 3. Change of projection velocity and dimensionless velocity with droplet radius

Controlling the velocity and direction of the projection by changing the shape of the bowstring

Fig. 4 shows how to control the projection velocity and direction by changing the shape of the bowstring (see Video S2-S5). When the bowstring is stretched (case 1→case 5→case 2, case 4→case 3), the projection velocity increases with the bowstring deformation increases, thus the maximum projection height increases, and the stagnation time after departure increases. By changing the angle of the bowstring (case 1, case 2, case 3→case 4→case 5), the liquid metal projectile can be projection in the expected direction.

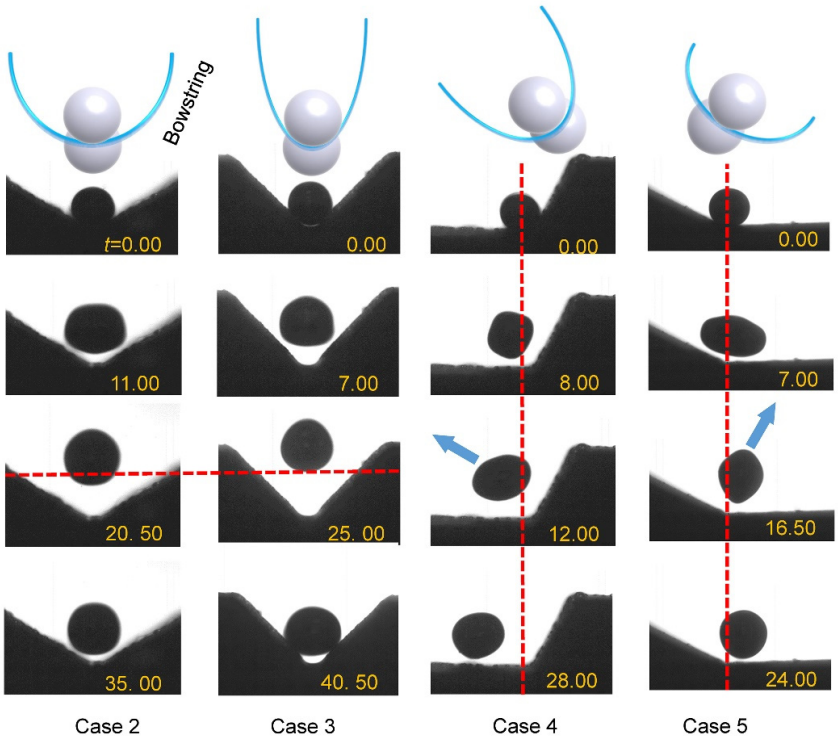

Fig. 4. The effect of bowstring shape on projection velocity and direction. Two equal-sized liquid metal droplets are placed back and forth to coalescence and induce the firing. The angle between the two bowstrings in case 2 and case 3 is 120° and 90°, and the bisector of the two bowstrings is perpendicular to the substrate. The angle between the two bowstrings in case 4 and case 5 is 120° and 150°, and the angle between the bisector and the substrate is 120° and 60°.

Fig. 5a shows the relationship between the amount of energy stored by the bowstring and the shape of the bowstring. The angle between the two bowstrings changes from 180° in case 1 to 90 ° in case 3, and the contact point between the single liquid metal droplet and the substrate changes from one to two. Thus both the contact area and the energy stored by the bowstring double. The contact area of case 5, case 2, and case 4 can be obtained by *Eq*.(5), and the surface energy and projection kinetic energy also increase with the elongation of the bowstring. Besides the increase of the energy stored in the bowstring, the elongation of the bowstring increases the ratio of the released surface energy to the projection kinetic energy, and then increase the projection velocity. Although the shape of bowstring has changed, *Eq*.(7) can still be used to predict the projection velocity. The values of C_0 corresponding to the bowstring angle of 180 °, 150 °, 120 °, 90 ° are 0.47, 0.55, 0.73, 0.90. Liquid metal droplets fire under the reaction force of bowstring, so changing the bowstring shape can control the projection direction. Assuming that the components of the force exerted by a single bowstring on the liquid metal in the horizontal and vertical directions are $F\sin(\theta_b)$ and $F\cos(\theta_b)$, where θ_b is the angle between the bowstring and the horizontal direction, the direction of the resultant force of the two bowstrings is:

$$\theta_p = \text{atan}\left(\frac{\cos(\theta_{b1})+\cos(\theta_{b2})}{\left|\sin(\theta_{b1})-\sin(\theta_{b2})\right|}\right) \tag{8}$$

where θ_p is the projection direction, θ_{b1} and θ_{b2} are the angle between the two bowstrings and the horizontal direction. As shown in Fig. 5b, the theoretical projection direction of case 1~5 are 90 °, 90 °, 90 °, 120 °, 75 ° respectively, and the experimental and theoretical values are consistent.

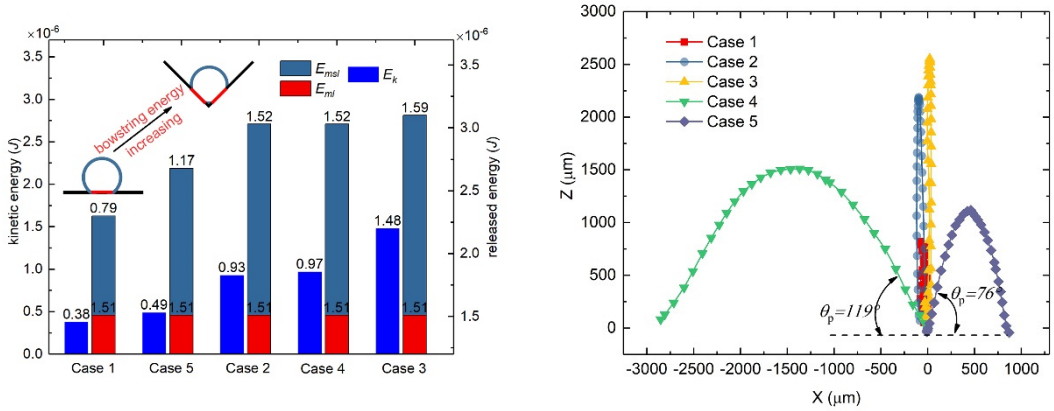

(a) (b)

Fig. 5. (a) The relationship between projection kinetic energy, bowstring energy, and bowstring shape. The calculation of kinetic energy takes the average projection velocity of three experiments for each case. (b) The relationship between the projection direction and the shape of the bowstring. Case 1 is the case shown in Fig. 1. The radii of droplets are 842 μm in all cases and the substrate

material Al-FAS.

CONCLUSION

In summary, we report a new self-proplled motion of liquid metal droplets, and we can adjust the projection velocity and direction by changing the shape of the bowstring like a slingshot, which is of great significance for the application of liquid metal. The present research is only a preliminary discovery of a kind of motion of liquid metal droplet, and no more systematic research has been carried out, such as the proportion, number, distribution, pH value of solution, solute, solvent, liquid metal alloy ratio, alloy type, interaction coupling between the substrate and the droplets double electric layer and others.

Beside, There are many kinds of liquid motion driven by surface tension, but most of their mechanisms are similar[33]. The firing of liquid metal droplets is very similar to the self-propelled jumping of water droplets in form, both of which induced by coalescence. The phenomenon of self-propelled water droplet jumping has been a research hotspot since it was found in 2009, and there are still many mechanical problems to be studied [32]. the research on how to control the direction[19] [24] and improve the jumping speed[25] is just beginning. Therefore, we cannot fully and clearly explain the similarities and differences between liquid metal droplet slingshot and self-propelled jumping of water droplets. However, it is obvious that the surfaces studied in this paper are all hydrophilic, it is impossible to have self-propelled jumping on such surfaces.

ACKNOWLEDGMENTS

This work was supported by the National Natural Science Foundation of China (No. 51976098), and the National Natural Science Foundation of China under Key Project (No. 91748206).

REFERENCES

1. Dickey, M. D., Stretchable and Soft Electronics using Liquid Metals. *Advanced Materials* **2017,** *29* (27), 19.

2. Yao, Y. Y.; Ding, Y. J.; Li, H. P.; Chen, S.; Guo, R.; Liu, J., Multi-Substrate Liquid Metal Circuits Printing via Superhydrophobic Coating and Adhesive Patterning. *Advanced Engineering Materials* **2019,** *21* (7), 1801363.

3. Todaro, C. J.; Easton, M. A.; Qiu, D.; Zhang, D.; Bermingham, M. J.; Lui, E. W.; Brandt, M.; StJohn, D. H.; Qian, M., Grain structure control during metal 3D printing by high-intensity ultrasound. *Nature Communications* **2020,** *11* (1), 142.

4. Wang, D.; Gao, C.; Wang, W.; Sun, M.; Guo, B.; Xie, H.; He, Q., Shape-Transformable, Fusible Rodlike Swimming Liquid Metal Nanomachine. *ACS Nano* **2018,** *12* (10), 10212-10220.

5. Yu, Y.; Miyako, E., Recent Advances in Liquid Metal Manipulation toward Soft Robotics and Biotechnologies. *Chemistry - A European Journal* **2018,** *24* (38), 9456-9462.

6. Yuan, B.; Zhao, C.; Sun, X.; Liu, J., Liquid-Metal-Enhanced Wire Mesh as a Stiffness Variable Material for Making Soft Robotics. *Advanced Engineering Materials* **2019,** *21* (10), 1900530.

7. Seok, S.; Onal, C. D.; Cho, K. J.; Wood, R. J.; Rus, D.; Kim, S., Meshworm: A Peristaltic Soft Robot With Antagonistic Nickel Titanium Coil Actuators. *IEEE-ASME Trans. Mechatron.* **2013,** *18* (5), 1485-1497.

8. Hou, Y.; Chang, H.; Song, K.; Lu, C.; Zhang, P.; Wang, Y.; Wang, Q.; Rao, W.; Liu, J., Coloration of Liquid-Metal Soft Robots: From Silver-White to Iridescent. *ACS Applied Materials & Interfaces* **2018,** *10* (48), 41627-41636.
9. Hu, L.; Wang, L.; Ding, Y.; Zhan, S.; Liu, J., Manipulation of Liquid Metals on a Graphite Surface. *Adv Mater* **2016,** *28* (41), 9210-9217.
10. Pollack, M. G.; Fair, R. B.; Shenderov, A. D., Electrowetting-based actuation of liquid droplets for microfluidic applications. *Applied Physics Letters* **2000,** *77* (11), 1725-1726.
11. Zhao, X.; Xu, S.; Liu, J., Surface tension of liquid metal: role, mechanism and application. *Frontiers in Energy* **2017,** *11* (4), 535-567.
12. Zhang, X. D.; Yang, X. H.; Zhou, Y. X.; Rao, W.; Gao, J. Y.; Ding, Y. J.; Shu, Q. Q.; Liu, J., Experimental investigation of galinstan based minichannel cooling for high heat flux and large heat power thermal management. *Energy Conversion and Management* **2019,** *185*, 248-258.
13. Ma, K.; Liu, J., Liquid metal cooling in thermal management of computer chips. *Frontiers of Energy and Power Engineering in China* **2007,** *1* (4), 384-402.
14. Bo, G.; Ren, L.; Xu, X.; Du, Y.; Dou, S., Recent progress on liquid metals and their applications. *Advances in Physics: X* **2018,** *3* (1), 1446359.
15. Zhu, J. Y.; Tang, S.-Y.; Khoshmanesh, K.; Ghorbani, K., An Integrated Liquid Cooling System Based on Galinstan Liquid Metal Droplets. *ACS Applied Materials & Interfaces* **2016,** *8* (3), 2173-2180.
16. Hu, L.; Wang, H.; Wang, X.; Liu, X.; Guo, J.; Liu, J., Magnetic Liquid Metals Manipulated in the Three-Dimensional Free Space. *ACS Appl Mater Interfaces* **2019,** *11* (8), 8685-8692.
17. Jin, S. W.; Jeong, Y. R.; Park, H.; Keum, K.; Lee, G.; Lee, Y. H.; Lee, H.; Kim, M. S.; Ha, J. S., A Flexible Loudspeaker Using the Movement of Liquid Metal Induced by Electrochemically Controlled Interfacial Tension. *Small* **2019,** *15* (51), 1905263.
18. Wang, M. F.; Jin, M. J.; Jin, X. J.; Zuo, S. G., Modeling of movement of liquid metal droplets driven by an electric field. *Physical Chemistry Chemical Physics* **2017,** *19* (28), 18505-18513.
19. Liu, J.; Guo, H.; Zhang, B.; Qiao, S.; Shao, M.; Zhang, X.; Feng, X.; Li, Q.; Song, Y.; Jiang, L.; Wang, J., Guided Self-Propelled Leaping of Droplets On a Micro-Anisotropic Superhydrophobic Surface. *Angew. Chem., Int. Ed.* **2016,** *55*, 4265.
20. Ju, J.; Zheng, Y.; Jiang, L., Bioinspired one-dimensional materials for directional liquid transport. *Acc Chem Res* **2014,** *47* (8), 2342-52.
21. Chen, H.; Ran, T.; Gan, Y.; Zhou, J.; Zhang, Y.; Zhang, L.; Zhang, D.; Jiang, L., Ultrafast water harvesting and transport in hierarchical microchannels. *Nat Mater* **2018,** *17* (10), 935-942.
22. Zhang, M.; Zheng, Y., Bioinspired Structure Materials to Control Water-collecting Properties. *Materials Today: Proceedings* **2016,** *3* (2), 696-702.
23. Yuan, Z.; Wu, R.; Wu, X., Numerical simulations of multi-hop jumping on superhydrophobic surfaces. *International Journal of Heat and Mass Transfer* **2019,** *135*, 345-353.
24. Yan, X.; Zhang, L.; Sett, S.; Feng, L.; Zhao, C.; Huang, Z.; Vahabi, H.; Kota, A. K.; Chen, F.; Miljkovic, N., Droplet Jumping: Effects of Droplet Size, Surface Structure, Pinning, and Liquid Properties. *ACS Nano* **2019,** *13* (2), 1309-1323.
25. Yuan, Z.; Hu, Z.; Chu, F.; Wu, X., Enhanced and guided self-propelled jumping on the superhydrophobic surfaces with macrotexture. *Applied Physics Letters* **2019,** *115* (16), 163701.
26. Qu, X.; Boreyko, J. B.; Liu, F.; Agapov, R. L.; Lavrik, N. V.; Retterer, S. T.; Feng, J. J.; Collier, C. P.; Chen, C., Self-Propelled Sweeping Removal of Dropwise Condensate. *Appl. Phys. Lett.*

2015, *106*, 221601.
27. Chu, F.; Wu, X.; Wang, L., Dynamic Melting of Freezing Droplets on Ultraslippery Superhydrophobic Surfaces. *ACS Appl Mater Interfaces* **2017,** *9* (9), 8420-8425.
28. Chu, F.; Wu, X.; Wang, L., Meltwater Evolution during Defrosting on Superhydrophobic Surfaces. *Acs Applied Materials & Interfaces* **2018,** *10* (1), 1415-1421.
29. Guo, R.; Sun, X.; Yuan, B.; Wang, H.; Liu, J., Magnetic Liquid Metal (Fe-EGaIn) Based Multifunctional Electronics for Remote Self-Healing Materials, Degradable Electronics, and Thermal Transfer Printing. *Advanced Science* **2019,** *6* (20), 1901478.
30. Eggers, J.; Lister, J. R.; Stone, H. A., Coalescence of liquid drops. *Journal of Fluid Mechanics* **1999,** *401*, 293-310.
31. Bird, J. C.; Dhiman, R.; Kwon, H. M.; Varanasi, K. K., Reducing the contact time of a bouncing drop. *Nature* **2013,** *503* (7476), 385-8.
32. Boreyko, J. B.; Chen, C. H., Self-propelled dropwise condensate on superhydrophobic surfaces. *Physical Review Letters* **2009,** *103* (18), 184501.
33. Sun, Q.; Wang, D.; Li, Y.; Zhang, J.; Ye, S.; Cui, J.; Chen, L.; Wang, Z.; Butt, H.-J.; Vollmer, D.; Deng, X., Surface charge printing for programmed droplet transport. *Nature Materials* **2019**.